

Cyclotron Resonance of an Interacting Polaron Gas in a Quantum Well. Magneto-Plasmon-Phonon Mixing

S. N. Klimin and J. T. Devreese

Theoretische Fysica van de Vaste Stof,
Universiteit Antwerpen (U.I.A.), B-2610 Antwerpen, Belgium
(Dated: August 26, 2003)

Abstract

Cyclotron-resonance (CR) spectra of a gas of interacting polarons confined in a GaAs/AlAs quantum well are theoretically investigated taking into account the magneto-plasmon-phonon mixing and band nonparabolicity. Contributions of different magneto-plasmon-phonon modes to the total magneto-polaron coupling strength are investigated as a function of the electron density. It is concluded theoretically, that the resonant magneto-polaron coupling in a high-density GaAs/AlAs quantum well occurs near the GaAs TO-phonon frequency rather than near the GaAs LO-phonon frequency. Calculated CR spectra are in agreement with recent experimental data.

I. INTRODUCTION

The electron-LO-phonon interaction plays an important role in the optical properties of polar semiconductors and ionic crystals (see, for review, Refs. [1, 2, 3, 4, 5]). The application of an external magnetic field adds new features to the optical absorption spectra of these materials. When the cyclotron frequency ω_c is close to the LO-phonon frequency, resonant magneto-polaron coupling (i. e., anticrossing of zero-phonon and, e. g., one-phonon states of the polaron system) occurs [6]. Experiments on the cyclotron resonance (CR) in bulk [7] and quasi-2D [8, 9, 10] systems give clear evidence of this resonant magneto-polaron coupling. However, CR measurements on semiconductor quantum wells with high electron density [11, 12] reveal that the anticrossing occurs near the TO-phonon frequency rather than near the LO-phonon frequency. In Ref. [12], on the basis of a model dielectric function for a 3D medium, it was suggested that in a GaAs/AlAs quantum well with high electron density, there may exist longitudinal modes, with energies close to the TO-phonon frequency, which are active in CR.

Another consequence of high electron densities combined with the nonparabolicity of the conduction band is a splitting of the CR lines [13, 14, 15, 16, 17]. It was shown in Ref. [16], that the one-particle approximation fails to interpret the oscillator strengths of the split CR lines.

Many-polaron CR in a 2D polaron gas was investigated theoretically in Ref. [18] using the memory-function technique [19]. In Ref. [10], this technique was applied to a polaron gas in a quantum well. The CR spectra of polarons in a quantum well were calculated in Ref. [20] and applied in Refs. [21, 22] taking into account the electron-phonon interaction for both bulk-like and interface phonon modes. To quantitatively explain the CR data for a high-density polaron gas, as observed in Ref. [12], it is necessary to take into account many-body effects.

In the present paper, the CR spectra of an arbitrary-density polaron gas in a quantum well are calculated using the many-body memory-function technique [19]. The approach developed in Refs. [18, 20] is extended here to a system of electrons confined in a quantum well and interacting with magneto-plasmon-phonon modes. Within this method, we take into account the electron-electron interaction, the static and dynamic screening of the electron-phonon interaction [18], the magneto-plasmon-phonon mixing [23], the band nonparabolicity and the phonon spectra specific for a quantum well.

The paper is organized as follows. In Sec. II, the optical conductivity for a polaron gas in a quantum well is derived. In Sec. III, we discuss the calculated CR spectra and compare them with experimental data for a GaAs/AlAs quantum well. Sec. IV contains the conclusions.

II. THEORETICAL APPROACH

A. Hamiltonian

We consider a finite-barrier quantum well of width d : The quantum well (medium 1) with high-frequency dielectric constant ϵ_1 is placed into a matrix (medium 2) with high-frequency dielectric constant ϵ_2 : Both these media are supposed to be polar. An external magnetic field B is applied parallel to the z -axis. The symmetric gauge is chosen for the vector potential

of the magnetic field,

$$\mathbf{A}(\mathbf{r}) = \frac{1}{2} [\mathbf{r} \times \mathbf{B}]: \quad (1)$$

The Hamiltonian describing the system, which consists of electrons interacting with phonons and with each other, is

$$\begin{aligned} H = & \sum_{n, \mathbf{l}m} E_{n, \mathbf{l}} a_{n, \mathbf{l}m}^{\dagger} a_{n, \mathbf{l}m} + \sum_{\mathbf{q}} \hbar \omega_{\mathbf{q}} b_{\mathbf{q}}^{\dagger} b_{\mathbf{q}} \\ & + \frac{1}{S} \sum_{\mathbf{q}} \sum_{\mathbf{k}} \sum_{\mathbf{n}, \mathbf{k}} (a_{\mathbf{q}})_{\mathbf{n}, \mathbf{k}} \sum_{\mathbf{l}m} (q) b_{\mathbf{q}} + b_{\mathbf{q}}^{\dagger}; \\ & + \frac{1}{2S} \sum_{\mathbf{q}} \sum_{\mathbf{n}_1, \mathbf{k}_1} \sum_{\mathbf{n}_2, \mathbf{k}_2} V_C(\mathbf{k}_1; \mathbf{n}_1; \mathbf{n}_2; \mathbf{k}_2; \mathbf{q}) N_{\mathbf{k}_1, \mathbf{n}_1}^{\dagger}(\mathbf{q}) N_{\mathbf{n}_2, \mathbf{k}_2}(\mathbf{q}); \end{aligned} \quad (2)$$

where $a_{n, \mathbf{l}m}^{\dagger}$ ($a_{n, \mathbf{l}m}$) is a creation (annihilation) operator for an electron in the one-particle state with energy $E_{n, \mathbf{l}}$ and with the wave function

$$\begin{aligned} \psi_{n, \mathbf{l}m}(\mathbf{r}; \mathbf{r}'; z) &= \psi_n(z) \phi_{\mathbf{l}m}(\mathbf{r}; \mathbf{r}'); \\ \phi_{\mathbf{l}m}(\mathbf{r}; \mathbf{r}') &= \frac{1}{2} e^{i \mathbf{m} \cdot \mathbf{r}'} \phi_{\mathbf{l}m}(\mathbf{r}); \end{aligned} \quad (3)$$

Here, the function $\psi_n(z)$ corresponds to the n -th size-quantized subband for motion along the z -axis, while $\phi_{\mathbf{l}m}(\mathbf{r}; \mathbf{r}')$ characterizes the "in-plane" motion of an electron with a definite z -projection m of its angular momentum, \mathbf{l} is the Landau level quantum number.

The phonon frequencies $\omega_{\mathbf{q}}$ and the amplitudes of the electron-phonon interaction $(a_{\mathbf{q}})_{\mathbf{n}, \mathbf{k}}$ are explicitly derived in Refs. [20, 30]. The index \mathbf{q} refers to the phonon branches, \mathbf{q} is the phonon two-dimensional wave vector, $b_{\mathbf{q}}^{\dagger}$ ($b_{\mathbf{q}}$) is a phonon creation (annihilation) operator. $N_{\mathbf{n}, \mathbf{k}}(\mathbf{q})$ is the electron density operator

$$N_{\mathbf{n}, \mathbf{k}}(\mathbf{q}) = \sum_{\mathbf{l}m, \mathbf{l}'m'} e^{i \mathbf{q} \cdot \mathbf{r}} \phi_{\mathbf{l}m, \mathbf{l}'m'}^{\dagger} a_{n, \mathbf{l}m}^{\dagger} a_{n, \mathbf{l}'m'} \quad (4)$$

with the matrix element

$$e^{i \mathbf{q} \cdot \mathbf{r}} \phi_{\mathbf{l}m, \mathbf{l}'m'}^{\dagger} = \int_0^{Z_1} dz \int_0^{Z_2} dz' e^{i \mathbf{q} \cdot \mathbf{r}} \psi_{\mathbf{l}m}(\mathbf{r}; \mathbf{r}') \psi_{\mathbf{l}'m'}^{\dagger}(\mathbf{r}; \mathbf{r}'); \quad (5)$$

In the Hamiltonian (2), $V_C(\mathbf{k}_1; \mathbf{n}_1; \mathbf{n}_2; \mathbf{k}_2; \mathbf{q})$ is the matrix element of the electron-electron interaction potential

$$V_C(\mathbf{k}_1; \mathbf{n}_1; \mathbf{n}_2; \mathbf{k}_2; \mathbf{q}) = \int_0^{Z_1} dz \int_0^{Z_1} dz' V_C(\mathbf{q}; z; z') \psi_{\mathbf{k}_1}(\mathbf{z}) \psi_{\mathbf{n}_1}(\mathbf{z}) \psi_{\mathbf{n}_2}^{\dagger}(z') \psi_{\mathbf{k}_2}^{\dagger}(z'); \quad (6)$$

S is the area of the quantum well in the xy -plane, $N[\cdot \cdot \cdot]$ is a normal product of operators. The two-dimensional Fourier amplitude $V_C(\mathbf{q}; z; z')$ of the electron-electron interaction potential, specific for the quantum well, differs from the corresponding expression for the Coulomb potential in bulk owing to the presence of the electrostatic image forces, which appear as long as $\epsilon_1 \neq \epsilon_2$ (see, e.g., Refs. [27, 28, 29]).

Within the local parabolic band approximation [24, 25], nonparabolicity is considered as a small perturbation. Consequently, the wave function $\psi_m(\mathbf{r})$ for an electron in a magnetic field takes the form

$$\psi_m(\mathbf{r}) = \frac{S}{(j_n j + K)!} \frac{m_b! c}{2\omega}^{\frac{j_n j + 1}{2}} j_n j \exp \left[-\frac{m_b! c}{4\omega} z^2 \right] L_K^{(j_n j)} \frac{m_b! c}{2\omega} z; \quad (7)$$

$$K = 1 - \frac{m + j_n j}{2}; \quad m = -1, \dots, 1$$

with the Laguerre polynomial $L_K^{(a)}(z)$. Here, the cyclotron frequency $\omega_c = eB = (m_b c)$ corresponds to the mass m_b given by [20]

$$m_b = \frac{m_{b1} m_{b2}}{P_w m_{b2} + P_b m_{b1}}; \quad (8)$$

where P_w (P_b) is the probability to find the electron inside (outside) the quantum well, and m_{bi} ($i = 1, 2$) is the electron band mass at the bottom of the conduction band in the i -th medium. The energies of the spin-dependent electron states are

$$E_{n1} = E_{n1} + g_B B; \quad (9)$$

where g is the Lande factor, B is the Bohr magneton, $s = \pm 1/2$ is the spin projection. The energy levels E_{n1} corresponding to the wave functions $\psi_{n1}(\mathbf{r}; z)$ in (3) are calculated using the k -p model [26].

B. Optical conductivity

Within the memory-function formalism, the real part of the frequency-dependent conductivity (in the Faraday configuration) in the local parabolic band approximation, can be written as [18, 25]

$$\text{Re}(\sigma(\omega)) = \frac{n_s e^2}{m_b} \text{Im} \frac{1}{\omega - \omega_c \frac{1}{\omega} (\omega; \omega_c) = \omega + i} \quad (\omega \rightarrow +0); \quad (10)$$

where n_s is the 2D electron density, and $\chi(\omega)$ is the memory function [18]. To take into account the splitting of the CR peaks due to the nonparabolicity of the conduction band, Eq. (10) is generalized as follows:

$$\text{Re}(\sigma(\omega)) = \sum_{n1} \chi_{n1} \text{Re}(\sigma_{n1}(\omega)); \quad (11)$$

where each contribution $\chi_{n1}(\omega)$, corresponding to the transitions $(l \rightarrow l+1)$,

$$\chi_{n1}(\omega) = \frac{n_s e^2}{m_b} \text{Im} \frac{1}{\omega - \omega_c^{(n1)} \frac{1}{\omega} (\omega; \omega_c^{(n1)}) = \omega + i} \quad (\omega \rightarrow +0) \quad (12)$$

is calculated with the local parabolic band approximation. The transition frequency

$$\omega_c^{(n1)} = \frac{E_{n1+1} - E_{n1}}{\hbar} \quad (13)$$

is used in Eq. (12) as distinct from the cyclotron frequency ω_c in Eq. (10). The weight $\{_{nl}$ is proportional to the number of open channels for the transitions $(l \rightarrow l+1)$. The normalized weights $\{_{nl}$ are

$$\{_{nl} = \frac{f_{nl} (1 - f_{n,l+1})}{\sum_{n',l'; 0} f_{n'l'0} (1 - f_{n',l'+1})}; \quad (14)$$

where f_{nl} is the Fermi occupation number. The memory function $\Gamma(\omega; \omega_c)$ takes the form (cf. Refs. [18, 20])

$$\begin{aligned} \Gamma(\omega; \omega_c) = & \sum_{n,k} \sum_{n',k'} \int \frac{d^2 q}{(2\pi)^2} \frac{(\epsilon_{nq})_{nk}^2 q^2}{n_S m_b^2(q)} \\ & \int_0^t dt e^{i\omega t} [1 - \text{Im} D(q;t) G_{nk}(q;t)] \quad (\omega \neq 0); \end{aligned} \quad (15)$$

where $\epsilon(q)$ is the static screening factor [18], $D(q;t)$ is the phonon Green's function

$$D(q;t) = i(t) b_{nq}(t) b_{nq}^+(0) + b_{nq}^+(t) b_{nq}(0) \quad (16)$$

and $G_{nk}(q;t)$ is the electron density-density Green's function

$$G_{nk}(q;t) = i(t) \frac{1}{S} \sum_{n,k} G_{nk}(q;t) + \sum_{n,k} G_{nk}(q;0) \quad (17)$$

with the Heaviside step function $\theta(t)$. The averaging in Eqs. (16) and (17) is performed on the equilibrium statistical operator of the electron-phonon system.

In the present paper, we apply the method presented above to the case of a GaAs/AlAs quantum well, where the weak-coupling regime is realized. To obtain $\Gamma(\omega; \omega_c)$ to second order in perturbation theory, the electron density-density Green's function $G_{nk}(q;t)$ can be calculated neglecting the electron-phonon interaction. The electron-electron interaction is taken into account in the random-phase approximation (RPA) following Ref. [31], where plasmon modes are derived for electrons in a layer. As a result, we arrive at the following set of equations in the Fourier representation

$$\sum_{n_1 k_1} [n_{n_1 k k_1} P_{nk}(q;!) V_C(k; n; k_1; n_1 !)] G_{n_1 k_1, nk}^R(q;!) = n_{n k} \sim P_{nk}(q;!); \quad (18)$$

Here, the auxiliary retarded Green's function $G_{nk, nk}^R(q;!)$ is determined as

$$G_{nk, nk}^R(q;!) = \frac{i}{S} \int_0^Z dt \sum_{n,k} G_{nk}(q;t) + \sum_{n,k} G_{nk}(q;0) e^{i\omega t} \quad (\omega \neq 0); \quad (19)$$

The RPA structure factor $P_{nk}(q;!)$ is proportional to the retarded density-density Green's function of non-interacting electrons in the quantum well in the presence of a magnetic field. It is calculated explicitly, using the second-quantization representation of the density operators (4), and takes the form

$$\begin{aligned} P_{nk}(q;!) = & \frac{m_b \omega_c}{2} \int_0^Z dt \exp[i(\omega - \omega_{kn})t] \sum_l L_l^{(0)} \frac{\omega_q^2}{m_b \omega_c} (1 - \cos \omega_c t) \\ & f_{n1} \exp \frac{\omega_q^2}{2m_b \omega_c} - 1 e^{i\omega_c t} - f_{k1} \exp \frac{\omega_q^2}{2m_b \omega_c} - 1 e^{i\omega_c t} \quad (20) \\ & (\omega \neq 0); \end{aligned}$$

where ω_{kn} is the transition frequency between the k -th and the n -th size-quantized subbands.

The set of equations (18) is valid for arbitrary electron density. The Green's function $G_{nk}(\mathbf{q}; \omega)$ is obtained from $G_{nk}^R(\mathbf{q}; \omega)$ using the Kramers-Kronig dispersion relations and the relation, which follows from the analytical properties of Green's functions,

$$\text{Im } G_{nk}^R(\mathbf{q}; \omega) = \frac{1}{2} e^{-\beta \hbar \omega} \text{Im } G_{nk}(\mathbf{q}; \omega); \quad (21)$$

where $\beta = 1/(k_B T)$. Further on, we consider the case of a sufficiently narrow quantum well, when only the lowest size-quantization subband ($n = 1$) is filled, and the transition frequency $\omega_{21} \approx \omega_{L1}$; where ω_{L1} is the LO-phonon frequency in the i -th medium ($i = 1, 2$). Under these conditions, transitions of an electron to other subbands can be neglected. This results in the explicit solution

$$G_{11}^R(\mathbf{q}; \omega) = \frac{\tilde{P}_{11}(\mathbf{q}; \omega)}{1 - V_C(\mathbf{q}) P_{11}(\mathbf{q}; \omega)} \quad (22)$$

with $V_C(\mathbf{q}) = V_C(1; 1; 1; 1; \mathbf{q})$:

The phonon retarded Green's function is calculated within the random-phase approximation taking into account the magneto-plasmon-phonon mixing (cf. Ref. [23]). In the present case of a narrow quantum well, we take into account the mixing of phonons with intrasubband magneto-plasmons only. In this approximation, disentangling a set of coupled Dyson equations leads to:

$$D^R(\mathbf{q}; \omega) = \frac{2\omega_{L1}^2 + \frac{j(\omega_{L1})^2}{\omega^2} G_{11}^R(\mathbf{q}; \omega)}{(\omega + i)^2 - \omega_{L1}^2 - 2\omega_{L1}^2 \frac{j(\omega_{L1})^2}{\omega^2} G_{11}^R(\mathbf{q}; \omega)} \quad (\omega \neq 0); \quad (23)$$

The poles of this Green's function are the roots of the equation

$$\omega^2 - \omega_{L1}^2 - 2\omega_{L1}^2 \frac{(\omega_{L1})^2}{\omega^2} \text{Re } G_{11}^R(\mathbf{q}; \omega) = 0 \quad (24)$$

and they determine the spectrum of mixed magneto-plasmon-phonon excitations in the quantum well. Let $\omega_{ij}(\mathbf{q})$ denote the positive roots of Eq. (24). Using $G_{11}^R(\mathbf{q}; \omega)$ given by Eq. (22), with the structure factor (20), we find that the retarded Green's function (23) can be expanded as a series

$$D^R(\mathbf{q}; \omega) = \sum_j A_{ij}(\mathbf{q}) \frac{1}{\omega - \omega_{ij}(\mathbf{q}) + i} - \frac{1}{\omega + \omega_{ij}(\mathbf{q}) + i}; \quad \omega \neq 0; \quad (25)$$

where $A_{ij}(\mathbf{q})$ is the residue of $D^R(\mathbf{q}; \omega)$ at $\omega = \omega_{ij}(\mathbf{q})$: The Green's function $D(\mathbf{q}; \omega)$ is obtained from $D^R(\mathbf{q}; \omega)$ using relations between $\text{Im } D^R(\mathbf{q}; \omega)$ and $\text{Im } D(\mathbf{q}; \omega)$ similar to Eq. (21), and the Kramers-Kronig dispersion relations. As a result, the Green's function $D(\mathbf{q}; \omega)$ can be written down explicitly,

$$D(\mathbf{q}; \omega) = \sum_j \frac{A_{ij}(\mathbf{q})}{1 - e^{-\beta \hbar \omega_{ij}(\mathbf{q})}} \frac{1}{\omega - \omega_{ij}(\mathbf{q}) + i} + \frac{e^{-\beta \hbar \omega_{ij}(\mathbf{q})}}{1 + \omega_{ij}(\mathbf{q}) + i}; \quad \omega \neq 0; \quad (26)$$

It is seen from Eqs. (15) and (26), that the parameter

$$w_{ij}(\mathbf{q}) = (\omega_{L1})^2 A_{ij}(\mathbf{q}) \quad (27)$$

determines the strength of the coupling between an electron and the $(i; j)$ -th magneto-plasmon-phonon mode characterized by the wave vector \mathbf{q} .

III. RESULTS AND DISCUSSION

Using the method developed in the previous section, the magneto-plasmon-phonon frequencies and the magneto-absorption spectra of a GaAs/AlAs quantum well are now calculated numerically. Within this approach, the CR peaks are proportional to delta-functions because of the discrete energy spectrum of an electron in a quantum well in the presence of a magnetic field (see, e.g., Ref. [20]). In what follows, we introduce in Eq. (15) a finite broadening of the Landau levels instead of the infinitesimal parameter $\delta \rightarrow 0$. Here, we choose the value $\delta = 0.01\Gamma_{L1}$, which corresponds to the linewidth of the CR peaks in the experiment of Ref. [12]. The material parameters used for the present calculation are listed in Table 1.

Table 1. Material parameters used for the calculation of the magneto-absorption spectra of a GaAs/AlAs quantum well

Parameter	GaAs	AlAs
LO-phonon energy, meV	36.3 [12]	50.09 [32]
TO-phonon energy, meV	33.6 [12]	44.88 [32]
Electron band mass, in units of the electron mass in the vacuum	0.0653 [26]	0.15 [32]
High-frequency dielectric constant	10.89 [32]	8.16 [32]
Electron-phonon coupling constant	0.068 [3]	0.148 [32]

The value 0.915 eV [20] is used for the AlAs/GaAs potential barrier. In the numerical calculation, we use a formula for the energy levels in a non-parabolic conduction band taken from Refs. [25, 26]

$$E_{n1} = \frac{E_0}{2} \left[1 + \sqrt{1 + 4 \frac{E_{n1}^0}{E_0}} \right]^{-1} \quad (28)$$

with the effective energy gap $E_0 = 0.98$ eV [26] and with $E_{n1}^0 = \hbar^2 c^2 (1 + \frac{1}{2} + n^2)$, where n is a size-quantized energy level characterizing the motion along the z -axis.

According to Ref. [20], the following phonon branches give contributions to the CR spectra in a quantum well: (i) bulk-like phonons with frequency ω_{L1} , (ii) symmetric interface phonons with frequencies ω_s ; (q) given by Eq. (7) of Ref. [20]. In a similar way, the magneto-plasmon-phonon modes in a quantum well can be classified into bulk-like and interface modes. The frequencies of these modes depend on the electron density and on the modulus q of the 2D wave vector q . As follows from our calculations, the modes, whose wave vectors lie in the region with $q \approx 2q_p$; where $q_p = (m_b \omega_{L1})^{1/2}$; give the dominant contribution to the magneto-optical absorption. In Fig. 1, frequencies of six mixed magneto-plasmon-phonon modes, which contribute significantly to the cyclotron-resonance spectrum, are plotted as a function of the electron density for $\omega_c = 0.8\omega_{L1}$ and for $q = 2q_p$. In the low-density limit, as seen from Fig. 1, the phonon modes do not mix with the magneto-plasmons. At $n_s \rightarrow 0$; the frequencies of the bulk-like and of two symmetric interface magneto-plasmon-phonon modes tend to ω_{L1} and ω_s ; (q), respectively (cf. Ref. [20]). With increasing density n_s ; the magneto-plasmon branch splits into three modes (shown by black curves). When the density

risers further, anticrossing of phonon and magneto-plasmon frequencies is to be expected between $10^{11} \text{ cm}^{-2} \leq n_s \leq 10^{12} \text{ cm}^{-2}$. This anticrossing allows us to distinguish between the lower-frequency modes (black curves) and the higher-frequency modes (red curves). Finally, for $n_s \approx 10^{12} \text{ cm}^{-2}$, the three higher frequencies tend to the magneto-plasmon frequency, which behaves as $\omega_s^{1=2}$; and the three lower frequencies are close to ω_{T1} and to $\omega_{S; (q)}$, respectively. The latter two magneto-plasmon-phonon frequencies are actually slightly reduced with respect to $\omega_{S; (q)}$. The appearance of the branch with frequency close to ω_{T1} instead of ω_{L1} is due to the screening of the electron-phonon interaction by the plasma vibrations.

In Fig. 2, the relative contributions of different magneto-plasmon-phonon modes to the total magneto-polaron coupling strength

$$w_{ij}(q) = \frac{w_{ij}(q)}{\sum_{ij} w_{ij}(q)} \quad (29)$$

are plotted as a function of n_s for $q = 2q_0$. In the low-density limit, the plasma vibrations give a vanishing contribution to $w_{ij}(q)$. In this case, the electrons interact only with phonons. For increasing electron density, the strength of the interaction of an electron with the lower-frequency magneto-plasmon-phonon modes rises, while that for the higher-frequency modes decreases. For a 10-nm GaAs/AlAs quantum well, the contribution of the interface magneto-plasmon-phonon modes into the CR spectra is smaller than that of the bulk-like modes. Nevertheless, the interaction of an electron with the interface modes is not negligible.

It was noted in Refs. [33, 34], that the participation of a magneto-plasmon at $q \neq 0$ in CR for a purely electronic system in a quantum well, without impurities, is not allowed by momentum conservation. However, for a polaron gas in a quantum well, the interaction of the electrons with the magneto-plasmon-phonon modes characterized in Fig. 2 is reflected in the CR spectrum. It is remarkable that, in the high-density limit, the largest coupling strength occurs for the mixed magneto-plasmon-phonon mode with ω_{T1} : This fact provides a quantitative basis for the understanding of the resonant magneto-polaron coupling observed in Ref. [12]. A related effect appears also for the magneto-phonon resonance: as shown in Ref. [35], the magneto-plasmon-phonon mixing leads to a shift of the resonant frequency of the magneto-phonon resonance in quantum wells from ω_{L1} to ω_{T1} .

In Ref. [12], CR spectra are measured for the absolute transmission $T(\omega)$; which is related to the optical absorption coefficient by

$$T(\omega) = 1 - \alpha(\omega) \quad (30)$$

The optical absorption coefficient is proportional to $\text{Re}(\epsilon(\omega))$,

$$\alpha(\omega) = \frac{4}{cn(\omega)} \text{Re}(\epsilon(\omega)); \quad (31)$$

where $n(\omega)$ is the refractive index. In Fig. 3, we compare the experimental [12] transmission spectra with the transmission spectra calculated in the present work for a polaron gas with electron density $n_s = 1.28 \times 10^{12} \text{ cm}^{-2}$ in a 10-nm GaAs/AlAs quantum well. Reliable comparison of our theoretical results with the experimental data of Ref. [12] can be performed only outside a frequency band near ω_{T1} (shown in Fig. 3 by the cross-hatched

area), because the experimental spectra in this frequency region are obtained after the elimination of a strong absorption peak due to direct TO-phonon absorption in the substrate. It is not straightforward to extract information on the CR spectra in this frequency region. It is seen from Fig. 3, that outside the cross-hatched area the theoretical peak positions of the magneto-transmission spectra calculated in the present work reasonably compare with the experimental data of Ref. [12]. If one tunes the magnetic field within the error bar, the agreement between theory and experiment can be improved. The remaining difference between theoretical and experimental peak positions can be explained by possible deviation of the values of the band parameters (the electron band mass and the effective energy gap) in a GaAs/AlAs quantum well from those in bulk.

The effect of the magneto-plasmon-phonon mixing is clearly manifested in the CR spectra, as seen, e. g., from the plot corresponding to a magnetic field $B = 22.25$ T, for which $\omega_c = \omega_{T1} = 33.6$ meV. For this value of B , the intensities of the peaks below ω_{T1} and above ω_{T1} are comparable both in the experiment [12] and in the present theory. Such a behavior is typical for resonant magneto-polaron coupling near ω_{T1} rather than near ω_{L1} .

The splitting of the CR peaks manifested in Fig. 3 reflects the nonparabolicity of the conduction band. In the experimental CR spectra [12], the higher-frequency and lower-frequency components of the split peaks are denoted as A- resp. B-components. The higher-frequency component of each split peak corresponds to the transitions between the Landau levels $(0 \rightarrow 1)$, while the lower-frequency component corresponds to the transitions $(1 \rightarrow 2)$. With increasing magnetic field strength, the distance between Landau levels rises, so that the upper filled level ($l = 1$) becomes less populated. As a result, the relative intensity of the lower-frequency peak diminishes. It is shown in Ref. [16], that the observed relative oscillator strengths of the split CR peaks are not consistent with the one-particle theoretical picture. The one-particle theories (e. g., Refs. [36, 37]) overestimate the lower-frequency peak intensity as compared to experiment. In particular, for a filling factor $\nu = 3$; the one-particle approximation predicts $I_{(1 \rightarrow 2)} = I_{(0 \rightarrow 1)} = 2$, which contradicts the experimental CR data for high electron densities [16], where this ratio is close to 1. It is noteworthy, that for $\nu = 3$; the coefficients $\{c_{nl}\}$ given by (14) for $l = 0$ and for $l = 1$ are equal to each other, while the contributions $Re_{nl}(\omega)$ only slightly depend on the Landau level quantum number. Therefore, for $\nu = 3$; our theory gives $I_{(1 \rightarrow 2)} = I_{(0 \rightarrow 1)} = 1$, in agreement with Ref. [16].

In Fig. 4, we plot a set of our theoretical magneto-absorption spectra for a GaAs/AlAs quantum well as a colormap. This map shows the magneto-absorption intensity as a function of both the magnetic field and the frequency. For comparison, the experimental peak position taken from Fig. 3 of Ref. [12] are shown in the same graph. For the peaks with $B / 17.2$ T (indicated by crosses) the splitting due to the band nonparabolicity is not resolved experimentally. It is seen from Fig. 4 that, for the high-density electron gas, anticrossing of the CR spectra occurs near ω_{T1} both for the experimental and for the calculated CR spectra. Starting from large B ; a set of peaks with $\omega > \omega_{T1}$ are pinned towards ω_{T1} from above, while starting from $B = 0$; another set of peaks are pinned from below to a frequency slightly larger than ω_{T1} :

For a low-density polaron gas in a GaAs/AlAs quantum well, it was found [20], that the resonance frequencies, calculated taking into account the interaction of electrons with both bulk-like and interface phonons, appreciably deviate from those found for the interaction with bulk LO phonons only. In particular, due to interface phonons, a resonance frequency appears between ω_{L1} and ω_{T1} (see Fig. 7 of Ref. [20]). In the present work, we take into

account, in addition to the effects due to the interaction of electrons with bulk-like and interface phonons, the many-body effects, which ensure the shift of the resonance frequency towards ω_{T1} ; when the electron density is high enough.

The splitting of the magneto-absorption peaks due to the band nonparabolicity, observed in the experiment for $\omega < \omega_{T1}$; continues in the theoretically calculated spectra also in the region $\omega > \omega_{T1}$. However, the intensity of the B-component for $\omega > \omega_{T1}$ is quite small.

IV . C O N C L U S I O N S

We have theoretically investigated cyclotron-resonance spectra for a polaron gas in a GaAs/AlAs quantum well with high electron density, taking into account (i) the electron-electron interaction and as a consequence the screening of the electron-phonon interaction, (ii) the magneto-plasmon-phonon mixing, (iii) the electron-phonon interaction with relevant phonon modes specific for the quantum well under consideration. As a result of the mixing, different magneto-plasmon-phonon modes appear in the quantum well and contribute to the CR spectra. In the 10-nm GaAs/AlAs quantum well (investigated experimentally in Ref. [12]), the interaction of an electron with the bulk-like modes is dominant. It is shown in the present work that, in the high-density polaron gas, the resonant magneto-polaron coupling, manifested in the CR spectra, takes place at a frequency close to the TO-phonon frequency in GaAs. This effect is in contrast with the cyclotron resonance of a low-density polaron gas in a quantum well, where anticrossing occurs near the LO-phonon frequency. Due to the band nonparabolicity, the CR spectrum of a high-density polaron gas in a quantum well is split into two components. The calculated CR spectra are in agreement with experiment, in particular, with the results of Ref. [12].

A c k n o w l e d g m e n t s

Discussions with V.M.Fomin, G.Martinez and V.N.Gladilin are gratefully acknowledged. This work has been supported by the GOA BOF UA 2000, IUAP., FWO-V. projects G.0274.01N, G.0435.03, the W.O.G.W.O.025.99 (Belgium) and the European Commission GROWTH Programme, NANOMAT project, contract No. G5RD-CT-2001-00545.

[*] Permanent address: Department of Theoretical Physics, State University of Moldova, str. A. Mateevici 60, MD-2009 Kishinev, Republic of Moldova.

[**] Also at: Universiteit Antwerpen (RUCA), Groenenborgerlaan 171, B-2020 Antwerpen, Belgium and Technische Universiteit Eindhoven, P.B. 513, 5600 MB Eindhoven, The Netherlands.

[1] Polarons and Excitons, edited by C.G.Kuper and G.D.Whitfield (Olivier and Boyd, Edinburgh, 1963)

[2] J.Appel, in: Solid State Physics, edited by F.Seitz, D.Tumbull, and H.Ehrenreich, Vol. 21, pp.193-391 (1968).

[3] Polarons in Ionic Crystals and Polar Semiconductors, edited by J.T.Devreese (North-Holland, Amsterdam, 1972).

[4] J.T.Devreese, in: Encyclopedia of Applied Physics (VCH, Weinheim, 1996), Vol. 14, p. 383.

- [5] P. Calvani, Optical Properties of Polarons (Editrice Compositori, Bologna, 2001).
- [6] D. Larsen, Phys. Rev. 135, A 419 (1964); in Ref. [3], p. 237.
- [7] B. D. McCombe and R. Kaplan, Phys. Rev. Lett. 21, 756 (1968).
- [8] Y.-H. Chang, B. D. McCombe, J.-M. Mercy, A. A. Reeder, J. Ralston and G. A. Wicks, Phys. Rev. Lett. 61, 1408 (1988).
- [9] J. P. Cheng, B. D. McCombe, and G. Brozak, Phys. Rev. B 43, 9324 (1991).
- [10] F. M. Peeters, X. Wu, J. T. Devreese, C. J. G. M. Langerak, J. Singleton, D. J. Barnes, and R. J. Nicholas, Phys. Rev. B 45, 4296 (1992).
- [11] M. Ziesmann, D. Heitmann, and L. L. Chang, Phys. Rev. B 35, 4541 (1987).
- [12] A. J. L. Poulter, J. Zeman, D. K. Maude, M. Potemski, G. Martinez, A. Riedel, R. Hey, and K. J. Friedland, Phys. Rev. Lett. 86, 336 (2001).
- [13] A. H. MacDonald and C. Kallin, Phys. Rev. B 40, 5795 (1989).
- [14] C. M. Hu, E. Batke, K. Kohler, and P. Ganser, Phys. Rev. Letters 75, 918 (1995).
- [15] C. M. Hu, T. Friedrich, E. Batke, K. Kohler, and P. Ganser, Phys. Rev. B 52, 12090 (1995).
- [16] M. Manger, E. Batke, R. Hey, K. J. Friedland, K. Kohler, and P. Ganser, Phys. Rev. B 63, 121203 (2001).
- [17] Yu. A. Bychkov and G. Martinez, Phys. Rev. B 66, 193312 (2002).
- [18] Wu Xiaoguang, F. M. Peeters, and J. T. Devreese, Phys. Rev. B 36, 9760 (1987).
- [19] H. Mori, Progr. Theor. Phys. 33, 423 (1965); 34, 399 (1965).
- [20] G. Q. Hai, F. M. Peeters, and J. T. Devreese, Phys. Rev. B 47, 10358 (1993).
- [21] Y. J. Wang, H. A. Nickel, B. D. McCombe, F. M. Peeters, J. M. Shi, G. Q. Hai, X.-G. Wu, T. J. Eustis, and W. Scha, Phys. Rev. Lett. 79, 3226 (1997).
- [22] J. T. Devreese and F. M. Peeters, in "High Magnetic Fields in Semiconductor Physics II", ed. by G. Landwehr, Springer Series in Solid-State Sciences Vol. 87 (Springer Verlag, Heidelberg, 1989).
- [23] L. Wendler and R. Pechstedt, J. Phys.: Condens. Matter 2, 8881 (1990).
- [24] D. Larsen, Phys. Rev. B 35, 9301 (1987).
- [25] X. Wu, F. M. Peeters, and J. T. Devreese, Phys. Rev. B 40, 4090 (1989).
- [26] P. Pfeiffer and W. Zawadzki, Phys. Rev. B 53, 12813 (1996).
- [27] E. P. Pokatilov, S. I. Beril, and V. M. Fomin, Phys. Stat. Sol. (b) 147, 163 (1988).
- [28] E. P. Pokatilov, S. I. Beril, V. M. Fomin, V. V. Kalinovskii, Phys. Stat. Sol. (b) 161, 603 (1990).
- [29] E. P. Pokatilov, V. M. Fomin, and S. I. Beril, Vibrational excitations, polarons and excitons in multilayer structures (Stiinta, Chisinau, 1990).
- [30] G. Q. Hai, F. M. Peeters, and J. T. Devreese, Phys. Rev. B 42, 11063 (1990).
- [31] W. H. Backes, F. M. Peeters, F. Brossens, and J. T. Devreese, Phys. Rev. B 45, 8437 (1992).
- [32] S. Adachi, J. Appl. Phys. 58, R1 (1985).
- [33] C. Kallin and B. I. Halperin, Phys. Rev. B 31, 3635 (1985).
- [34] B. Zhang, M. F. Manger, and E. Batke, Phys. Rev. Letters 89, 039703 (2002).
- [35] V. V. Afonin, V. L. Gurevich, and R. LaHo, Phys. Rev. B 62, 15913 (2000).
- [36] K. L. Kobayashi and E. Otsuka, J. Phys. Chem. Solids 35, 839 (1974).
- [37] T. Ando, J. Phys. Soc. Japan 38, 989 (1975).

Figure captions

Fig. 1 (color). Frequencies of magneto-plasmon-phonon modes in a 10-nm GaAs/AlAs quantum well as a function of the electron density. The value $\omega_c = 0.8\omega_{L1}$ is taken for the cyclotron frequency. Solid, dashed and dash-dotted curves correspond to bulk-like, interface (GaAs) and interface (AlAs) modes, respectively.

Fig. 2 (color). Relative contributions of six magneto-plasmon-phonon modes to the total magneto-polaron coupling strength $w(q) = \sum_j w_{ij}(q)$ in a 10-nm GaAs/AlAs quantum well as a function of the electron density. The other modes are neglected, because their relative contribution is only about 10^{-4} of $w(q)$. The notations are the same as those of Fig. 1.

Fig. 3 (color). Experimental and theoretical transmission spectra, at different magnetic fields, for a 10-nm GaAs/AlAs quantum well with electron density $n_s = 1.28 \times 10^{12} \text{ cm}^{-2}$. The black solid curves represent the experimental data of Ref. [12]. The red dashed curves correspond to the present theory.

Fig. 4 (color). Color map of the cyclotron resonance spectra for a 10-nm GaAs/AlAs quantum well. Symbols indicate the peak positions of the experimental spectra (which are taken from Fig. 3 of Ref. [12]). The dashed lines show LO- and TO-phonon frequencies in GaAs.

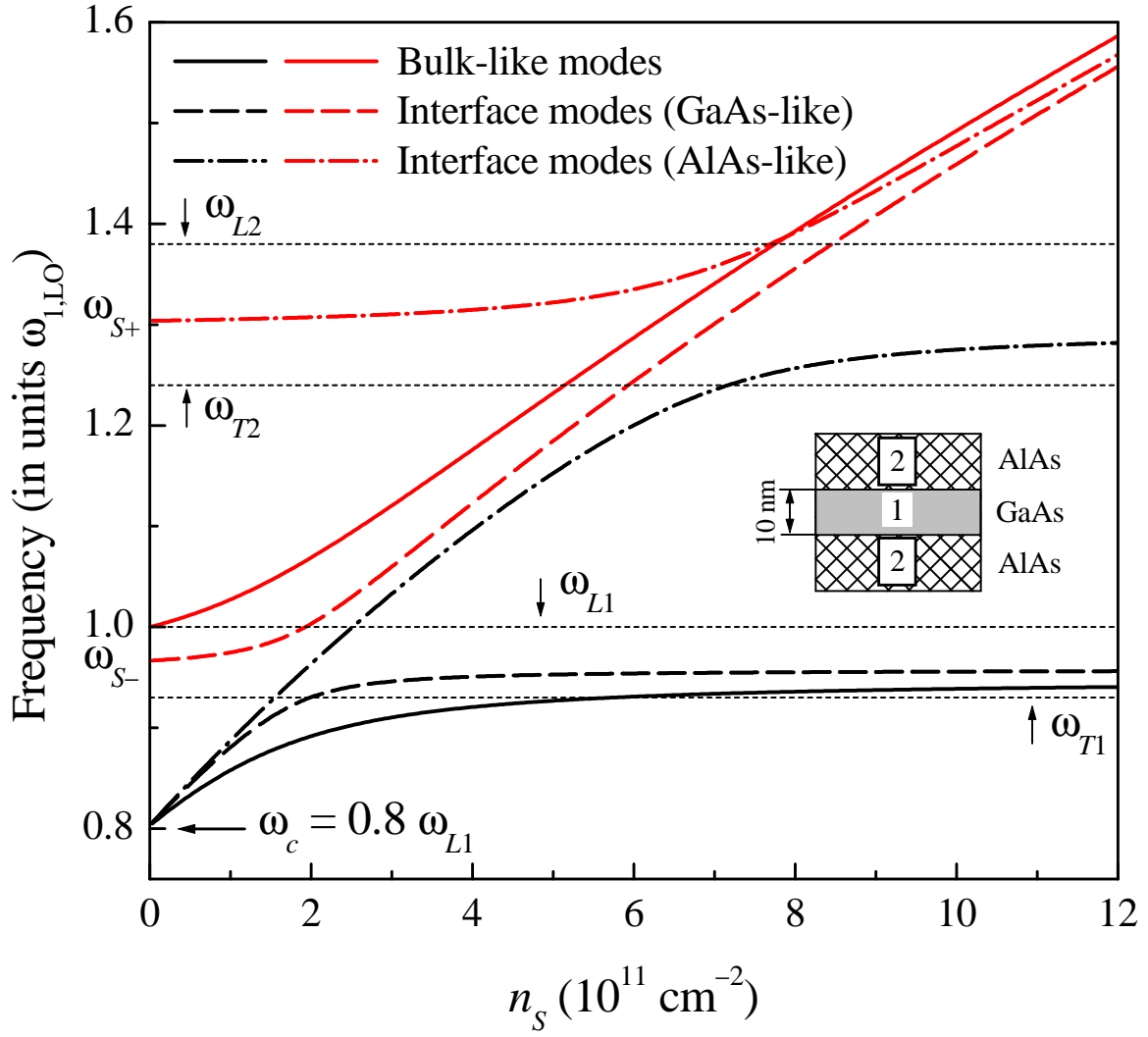


Fig. 1 S. N. Klimin and J. T. Devreese, Physical Review B

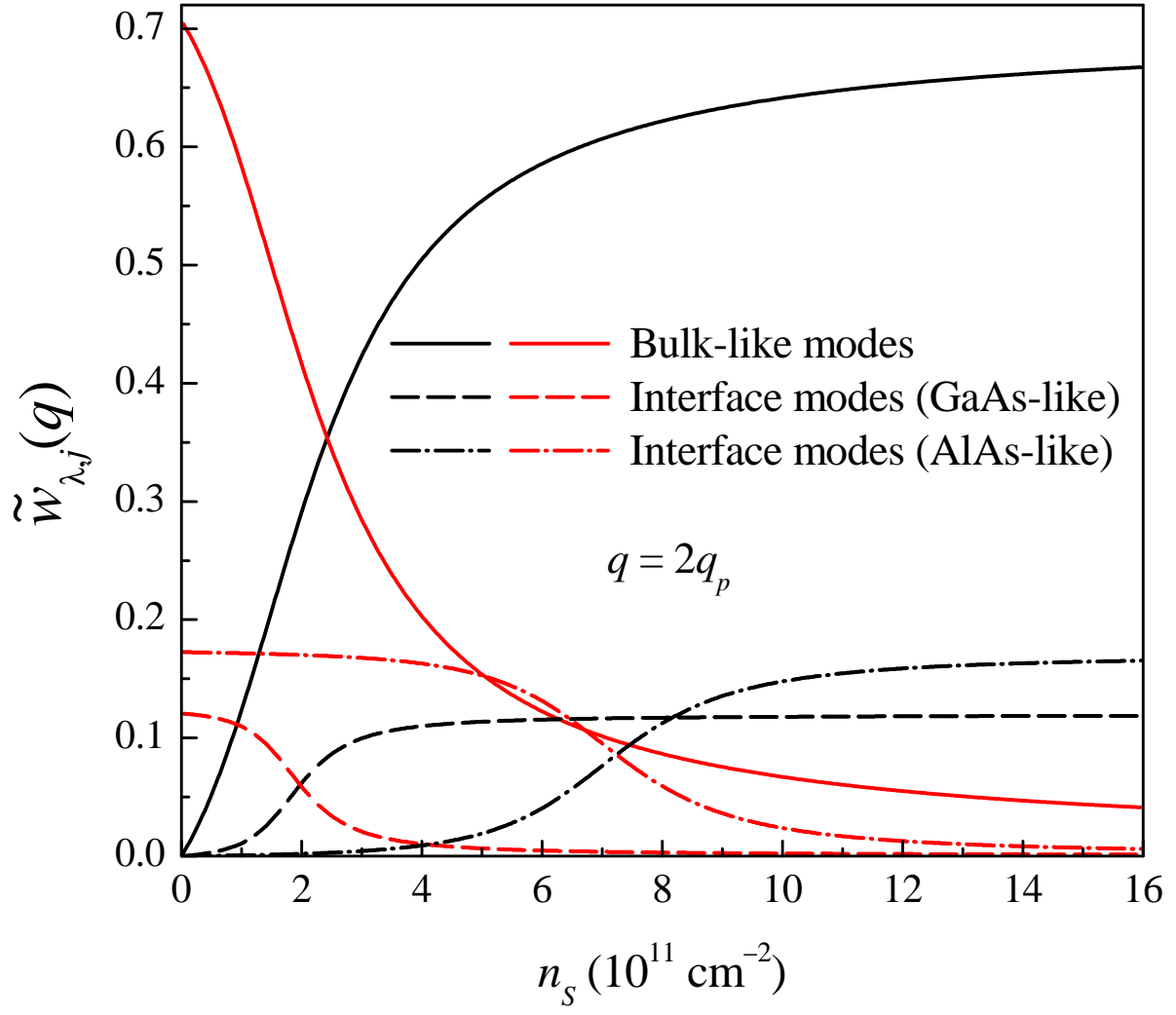


Fig. 2 S. N. Klimin and J. T. Devreese, Physical Review B

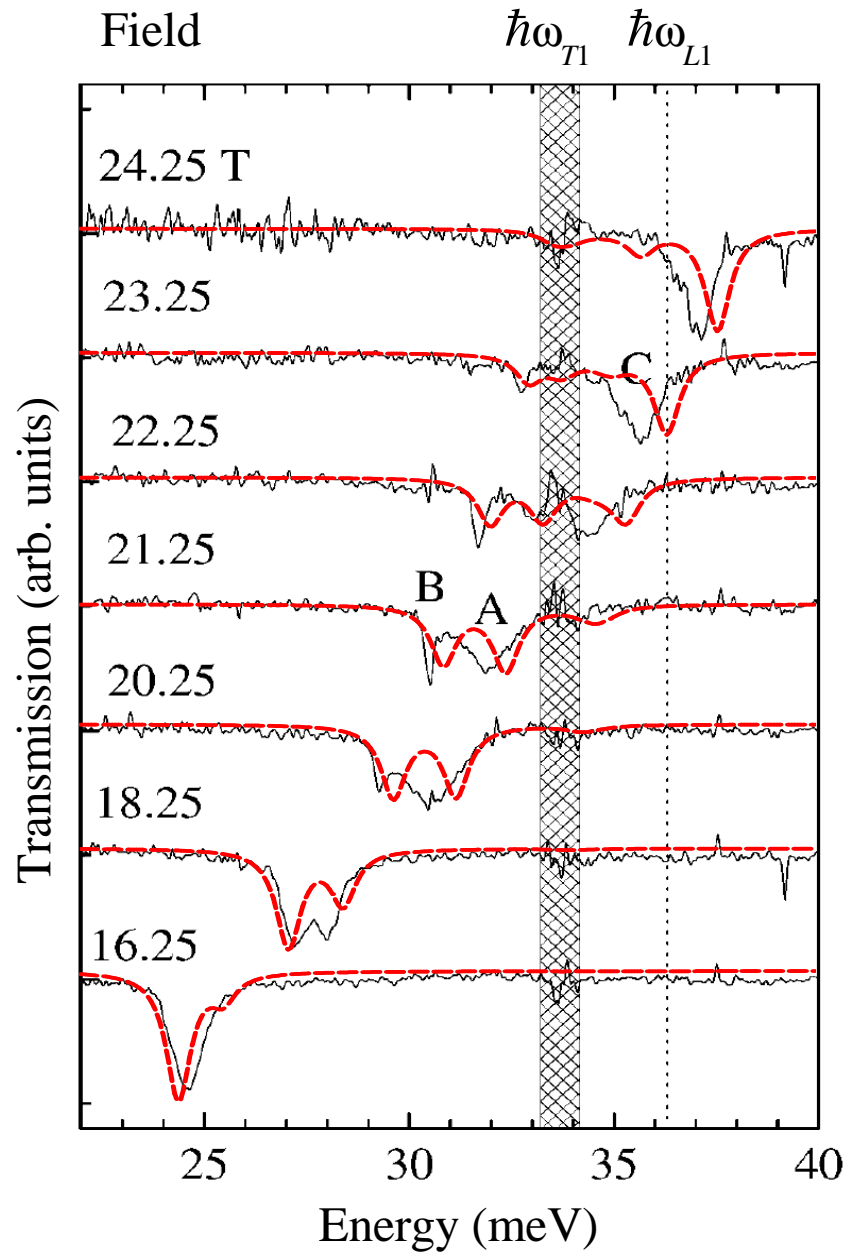


Fig. 3 S. N. Klimin and J. T. Devreese, Physical Review B

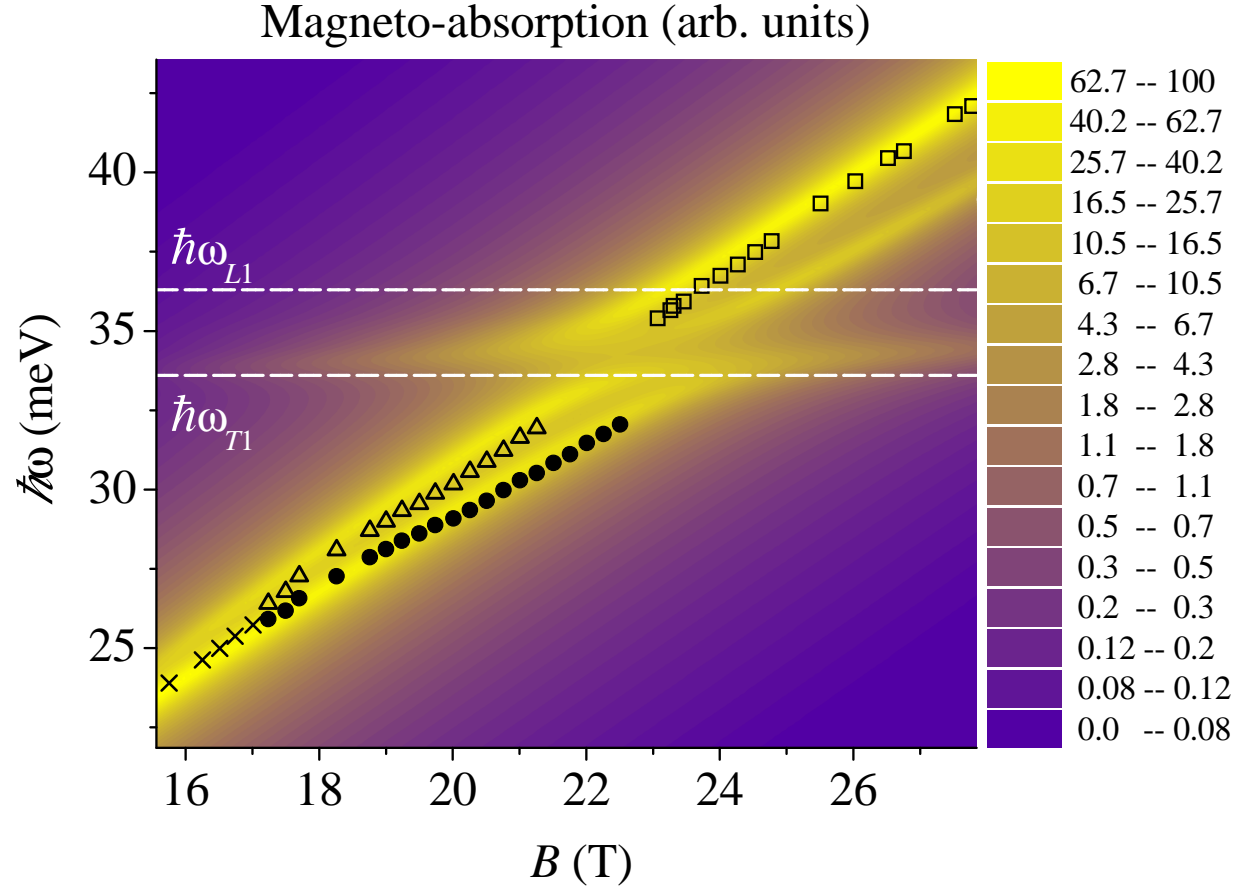


Fig. 4 S. N. Klimin and J. T. Devreese, Physical Review B